Neurochemical Research (2018) 43:1283–1296
https://doi.org/10.1007/s11064-018-2545-4

ORIGINAL PAPER

All-Trans Retinoic Acid Ameliorates the Early Experimental Cerebral Ischemia–Reperfusion Injury in Rats by Inhibiting the Loss of the Blood–Brain Barrier via the JNK/P38MAPK Signaling Pathway

Minghang Li[1] · Xiaocui Tian[1] · Ruidi An[1] · Mei Yang[1] · Qian Zhang[1] · Fei Xiang[1] · Hailin Liu[1] · Yuchun Wang[1] · Lu Xu[1] · Zhi Dong[1]

Received: 21 January 2018 / Revised: 9 April 2018 / Accepted: 16 April 2018 / Published online: 25 May 2018
© Springer Science+Business Media, LLC, part of Springer Nature 2018

Abstract

All-trans retinoic acid (ATRA) influences the outcomes of cerebral ischemic reperfusion (CIR) injury, but the mechanism remains unclear. The present study aimed to investigate the effects of ATRA on loss of the blood brain barrier (BBB) following CIR and to explore the possible mechanisms. Transient middle cerebral artery occlusion was performed on male SD rats to construct an in vivo CIR model. Neurological deficits, BBB permeability, brain edema, MRI and JNK/P38 MAPK proteins were detected at 24 h following CIR. We demonstrated that ATRA pretreatment could alleviate CIR-induced neurological deficits, increase of BBB permeability, infarct volume, degradation of tight junction proteins, inhibit MMP-9 protein expression and activity. ATRA treatment also reduced the p-P38 and p-JNK protein level. However the protective effect of ATRA on CIR could be reversed by administration of retinoic acid alpha receptor antagonist Ro41-5253. SP600125 and SB203580, which is the JNK/P38 pathway inhibitors has the same protective effect as ATRA. These results indicated that ATRA may inhibit the JNK/P38 MAPK pathway to alleviate BBB disruption and improve CIR outcomes.

Keywords All-trans retinoic acid · Blood–brain barrier · Cerebral ischemia–reperfusion · MMP-9 · JNK/P38 MAPK signaling pathway

Introduction

The blood–brain barrier (BBB) is a specialized interface between the blood and the central nervous system [1]. BBB acts as a transporting access supervision, and protects the central nervous system from harmful factors. Therefore, BBB plays an important role in maintaining the homeostasis of the brain environment. The structure of the BBB is primarily composed of brain microvascular endothelial cells (BMECs), basement membranes,and astrocyte end-feet and pericytes [2]. Studies have demonstrated that tight junction proteins (TJ) between specialized BMECs, consisting of several critical proteins such as claudin-5, occludin, and zonula occludens-1 (ZO-1), is an important structure to maintain BBB integrity and restrict paracellular permeability [3]. AQP-4 is known to increase swelling of the paws of astrocytes, increase permeability of the blood–brain barrier, and trigger significant cerebral edema and infarction. Disruption of the BBB has been observed following cerebral ischemic reperfusion (CIR) injury [4], which is accompanied by neuroinflammatory responses, oxidative stress and brain edema. BBB destruction ultimately contributes to neurological deficits, synaptic and neuronal dysfunction and cognitive changes. Several crucial proteins, including claudin-5, Occludin, ZO-1, were decreased after ischemia and reperfusion, which might cause the disruption of the BBB.

Matrix metalloproteinase-9 (MMP-9), which belongs to a family of zinc-binding proteolytic enzymes, involvs in BBB disruption in ischemic injury [5]. Upregulation of MMP-9 expression has been observed in the blood–brain barrier injury; [6, 7]. Previous study has also demostrated that MMP-9 impaired theintegrity of the BBB by cleaving TJs and the extracellular matrix [8]. Therefore, inhibition

✉ Lu Xu
xulu8792@163.com

✉ Zhi Dong
dongzhi5536@163.com

[1] Chongqing Key Laboratory of Biochemistry and Molecular Pharmacology, College of Pharmacy, Chongqing Medical University, District of Yuzhong, Chongqing 400016, China

overexpression of MMP-9 may be an important strategy to alleviate CIR injury.

Mitogen activated protein kinase (MAPK) pathway, including c-Jun N-terminal Kinase JNK pathway, P38 MAPK pathway and extracellular signal pathway (ERK) [9], is a key pathway involved in the protection of BBB. Recent studies have confirmed that in many tumors, cytokines and other extracellular stimulating factors can activate the MAPKs signaling pathway, up regulate the expression of MMP-9, and promote the invasion and metastasis of tumors [10]. Previous study have demonstrated that JNK and P38 are positivly involved in the inflammatory response, cytokines and cell proliferation after CIR [11].

ATRA is an active metabolite of vitamin A, which exerts most of the biological functions of vitamin A. ATRA has been widely used in the treatment of acute promyelocytic leukemia. ATRA binds to nuclear specific receptor to form ligand receptor complex, which participate in cell or tissue formation, enzymes involved in metabolism and regulation, and regulatory proteins that regulate the expression of lower genes [12]. Studies in tumor cells have found that ATRA promotes the expression of matrix metalloproteinase inhibitors (TIMPS), regulates the proportion of MMP/TIMP, and inhibits metastasis of tumor cells [13]. ATRA also plays a role in regulating immunity. It is also proved that ATRA can reduce the expression of oxidative stress products and NF-κB in liver ischemia–reperfusion injury [14–16]. However, the role of ATRA in BBB disruption in CIR remains virtually unclear and the relationship among ATAR among MMP-9 and MAPK signing pathway are poorly understood. In the current study, our purpose is to investigate whether ATRA treatment could ameliorate the loss of BBB integrity and understand the role of JNK/P38 MAPK Pathway in it.

Materials and Methods

All animal procedures were approved by the Experimental Ethics Committee of Chongqing Medical University in Chongqing, China. All experiments were performed in accordance with the experimental regulations of Chongqing Medical University. All surgeries were performed under anesthesia, and all efforts were made to minimize the animals' suffering.

Materials

Animals

A total of 120 male Sprague–Dawley rats weighing 270 ± 20 g in an individual ventilated cages (IVC) grade were obtained from the Experimental Animal Center of Chongqing Medical University (Chongqing, China). They were randomly divided into six groups (n = 20, in each group): the sham-operated group (Sham), the cerebral ischemia–reperfusion group (CIR), the ATRA-pretreated CIR group (low dose = 10 mg/kg, high dose = 30 mg/kg), the Ro41-5253 + ATRA-pretreated CIR group (Ro41-5253 + High dose, CIR + Ro + H), and SB203580 + SP600125-treated CIR group (CIR + SB + SP).

Middle Cerebral Artery Occlusion Model

Rats were anesthetized by 4% pentobarbital sodium (40 mg/kg, intraperitoneally). The right carotid artery (CCA), the external carotid artery (ECA) and the internal carotid artery (ICA) were separated from the right lateral sternocleidomastoid muscle and the anterior cervical muscle by supine fixation and the midline incision of the neck. Using Zea-Longa method [17], the vagus nerve improved four separate internal carotid artery and external carotid artery bifurcation, CCA ligation and ECA proximal internal carotid artery through the way of blocking the suspension line. Then, take a small cut at the CCA bifurcation 5 mm and feed the ICA wire bolt about 18 mm in length. The filament was withdrawn gently after 120 min of occlusion, and the brain was then reperfused 24 h. In the sham-operation subjects, nothing was inserted. Rats were put back to cages after recovery, with free access to tap water and food. Throughout the procedure, body temperature was maintained at 37 ± 0.5 °Cwith a thermostatically controlled infrared lamp.

Drug Administration

ATRA (Sigma-Aldrich Co. LLC, St. Louis, MO, USA) was dissolved in a 1:1 mixture ratio of v/v dimethyl sulfoxide (DMSO): saline (0.9% w/v sodium chloride) to prepare different concentrations of ATRA solutiong (10, 30 mg/kg) [18]. After operation, rats in the ATRA group respectivly received ATRA (10, 30 mg/kg) through intraperitoneal injection, group sham and group CIR rats were injected with equal amount of solvent. Ro41-5253 (0.5 mg/kg) was administered intravenously 30 min prior to ischemia. 10 µl SB203580 and 10 µl SP600125 (soluble at 1%DMSO, concentration 30 mg/ml) were injected into the lateral ventricles of the brain 30 min before the establishment of the model.

Neurologic Deficit

After 24 h of reperfusion, neurologic deficit was assessed by researchers who were unaware of the rats' group assignments (n = 11). The assessment was accomplished according to Longa 5 level 4 points method [19]. The criteria for scoring were as follows:

Grade 0: no nerve injury symptoms;

Grade 1: when the tail of the contralateral forelimb lesions can not be completely straight;

Grade 2: while walking to the paralyzed side around;

Grade 3: when walking to the contralateral falls;

Grade 4: can not walk spontaneously, loss of consciousness.

Infarct Volume

For quantification of cerebral infarct volume, rats in each group were sacrificed, and the mouse brains were quickly isolated, frozen and cut into four coronal sections with 2 mm thickness. The brain sections (1 mm) were incubated in 2% 2,3,5-triphenyltetrazolium chloride (TTC) at 37 °C for 15 min, and transferred to 4% paraformaldehyde overnight. Unstained areas were recognized as infarctions. The infarct volume was analyzed quantitatively using Image-pro Plus software and expressed as percentage of contralateral hemisphere. Infract volume (%) = (cerebral infarction area/whole brain area) × 100%.

Brain Water Content Calculations

Brain edema was detected using the wet/dry method as previously described [20]. The rats (n = 10) were anesthetized carefully and the brain was removed by decapitation. Briefly, the right brain was immediately removed and placed on saline-soaked filter paper to prevent evaporation, pia mater and blood were carefully removed, and weighed to obtain the wet weight. And then the brain tissue was subsequently placed in an oven at 105 °C for 24 h, followed by re-weighing to obtain the dry weight. Brain water content = [(wet weight − dry weight)/wet weight] × 100%.

Magnetic Resonance Imaging

At 24 h after I/R (n = 5), the MRI contrast agent Omniscan (1.5 ml/kg) was injected via caudal vein by a 1 ml syringe, and an advanced 1.5 T nuclear magnetic resonance system (Siemens) was used to detect and evaluate BBB disruption [21]. Precise MRI information was obtained from T1-weighted intensifier scanning. MRI signal data were collected by the MRI system software.

Evans Blue Method

To determine the effect of ATRA on BBB integrity, rats in each group were injected with 2% EB (4 ml/kg) via the caudal vein. At 24 h after CIR, infusion with heparinized saline through the left ventricle was performed until colorless infusion fluid was obtained from the right atrium; then, the rats were decapitated. The right hemisphere was weighed, placed in a tube with 3 ml dimethylformamide (DMF), and then thawed in water at 60 °C in a dark room for 24 h. The optical density (OD) value of EB was measured by a RF-540 fluorescence spectrophotometer (λ = 632 nm). The EB content was calculated from a standard EB curve to measure the change in BBB permeability.

Transmission Electron Microscopy

Ultrastructure of BBB was analyzed using TEM. Rats (n = 5) were deeply anesthetized and then fixed with 4% paraformaldehyde containing 1% glutaraldehyde by perfusion. The cortex region was sliced into cubes (1 mm^3), and then fixed in glutaraldehyde (2.5%) and 1% osmic acid for 4 h respectively. Specimens were dehydrated with acetone and embedded by Epon812. The ultrathin sections of the cubes were dyed with uranyl acetate and lead citrate, and then observed under transmission electron microscopy (TEM, Hitachi, 7100, Japan).

Immunofluorescence Staining

To characterize the expression of tight junction protein claudin-5 in ischemic region, rats in each group (n = 5) were sacrificed and brain tissue was rapidly isolated and post-fixed in 4% paraformaldehyde for 4 h, followed by overnight immersion in phosphate buffer containing 30% sucrose. The brains were then embedded in OCT solution, and 8 μm coronal brain cryosections were prepared. Sections were fixed in ice-cold acetone and blocked with 10% goat serum for 2 h. Next, the sections were incubated at 4 °C overnight with the following primary antibodies: rabbit anti-claudin-5 antibodies (1:100, bs-10296R, Bioss, BeiJing, China) at 4 °C overnight. After washed in PBS, the sections were incubated with appropriate secondary antibody for 30 min at 37 °C: DyLight 488 affiniPure goat anti-rabbit IgG (1:100, A23220, Abbkine, USA). Blood vessels were incubated with biotinylated Lycopersicon esculentum (tomato) Lectin (1:100 B-1175, Vector Laboratories, Burlingame, USA). Nuclei were stained with 4′,6-diamidino-2-phenylindole (DAPI, C1006, Beyotime, China). Images were captured with a fluorescence microscope (Eclipse Ti-S, Nikon, Japan), and visual fields per section were analyzed using Image-pro plus (IPP) 6.0 software.

Gelatin Zymography Assay

The right hemisphere samples (n = 10) were homogenized in lysis buffer including pro tease inhibitors at 50 mg/ml and then centrifuged at 12,000 rpm for 15 min at 4 °C. The activity of MMP-9 was assessed using a gelatin zymography kit according to the manufacturer's protocol

(GMS30071.1, Genmed Scientifics Inc. USA). MMP-9 activity was quantified by performing densitometric analyses with Bio-Rad Image Lab software 4.0 (Bio-Rad, Hercules, CA, USA).

Western Blotting

Anaesthetized rats (n = 12) were decapitated and the right brain tissues were rapidly extracted on ice, weighted and grinded in liquid nitrogen, then approximate 70 mg homogenates were weighted. These frozen tissue powder was transferred to a 1.5 ml centrifuge tube with RAPI lysis buffer (P00113D; Beyotime, Shanghai, China) that contained proteinase and phosphatase inhibitor cocktail. The homogenates were centrifuged at 12,000 g for 5 min at 4 °C and the supernatants were collected as total proteins. The protein samples were quantified with a bicinchoninic acid protein assay kit (P0012S, Beyotime, China). The protein was separated using sodium dodecyl sulfate-polyacrylamide gel electrophoresis (SDS-PAGE) (P0012A, Beyotime, China) with a 12% polyacrylamide gel, and then transferred to polyvinylidene fluoride (PVDF) membrane. Then the membranes were blocked with non-fat milk (5%) and incubated overnight at 4 °C with the following primary antibodies: rabbit polyclonal anti-Zo-1 (21773-1-AP, Proteintech, Wuhan, China, 1:500), rabbit polyclonal anti-claudin-5 (bs-10296R, Bioss, BeiJing, China, 1:500), rabbit polyclonal anti-occludin (13409-1-AP, Proteintech, Wuhan, China, 1:1000), rabbit polyclonal anti-MMP-9 (10375-2-AP, Proteintech, Wuhan, China, 1:1000), mouse monoclonal anti-Bax (60267-1-Ig, Proteintech, Wuhan, China,1:1000), rabbit polyclonal anti-Bcl-2 (ab59348, Abcam, Cambridge, UK,1:300),rabbit polyclonal anti-cleaved caspase 3 (#9664, Cell Signaling Technology, Beverly, MA, USA,1:500), rabbit polyclonal anti-AQP-4 (16473-1-AP, Proteintech, Wuhan, China,1:500), Goat polyclonal anti-RARα(ab28767, Abcam, Cambridge, UK,1:1000), rabbit polyclonal anti-JNK (10023-1-AP, Proteintech, Wuhan, China, 1:1000), rabbit polyclonal anti-P38 (14064-1-AP, Proteintech, Wuhan, China, 1:1000), rabbit polyclonal anti-Phospho-P38MAPK (Thr180/Tyr182) (D3F9) (#4511, Cell Signaling Technology, Beverly, MA, USA,1:1000), rabbit polyclonal anti-Phospho-SAPK/JNK (Thr183/Tyr185) (81E11) (#4668, Cell Signaling Technology, Beverly, MA, USA,1:1000) and rabbit polyclonal anti-β-actin (20536-1-AP, Proteintech, Wuhan, China,1:1000). After three washes, secondary antibodies Biotin-conjugated Affinipure Goat Anti-Mouse IgG (H + L) (SA00004-1, Proteintech, Wuhan, China, 1:2000), Biotin-conjugated Affinipure Goat Anti-Rabbit IgG (H + L) (SA00004-2, Proteintech, Wuhan, China, 1:2000), Biotin-conjugated Affinipure Donkey Anti-Goat IgG (H + L) (SA00004-3, Proteintech, Wuhan, China, 1:2000) were performed to conjugate with alkaline phosphatase for 2 h at room temperature. After three washes, thirdly antibody HRP-conjugated Streptavidin (SA00001-0, Proteintech, Wuhan, China, 1:3000) was performed to conjugate with alkaline phosphatase for 1 h at 37 °C. β-actin was used as an internal control. The immune bands were detected with an ECL kit (Advansta, Menlo Park, CA, USA). The density of each band was quantified using Image Lab software (Bio-Rad, Hercules, CA, USA).

Statistical Analysis

All data are presented as the mean ± SD. SPSS 17.0 was used to analyze the data between the groups with a one-way analysis of variance (ANOVA) test followed by the Tukey's test. A value of $P < 0.05$ was defined as statistically significant.

Results

ATRA Alleviates Focal Ischemia-Induced Brain Injury in Rats

We examined whether ATRA protects the brain aganist ischemia induced injury by 24 h of reperfusion after MCAO. As shown in Fig. 1c, severe neurological deficits were present in the CIR group, while ATRA treatment (10 and 30 mg/kg) reduced the neurological score, which suggests that ATRA treatment improves the functional outcome after CIR injury. Additionally, consecutive brain sections stained with TTC were also detected. Compared to the CIR group, ATRA treatment (10 and 30 mg/kg) decreased the total infarct volume from 5 to 8% respectively (Fig. 1a, b, $^{**}p < 0.01$). MRI approach was also used to determined the infract volume. A markedly increased T1-hyperintensity was observed with in rats undergoing CIR injury compared with the sham-operated group at 24 h. However, ATRA treatment (10 and 30 mg/kg) significantly attenuated T1 hyperintensity in comparison to the CIR group rats (Fig. 2a, b, $^{**}p < 0.01$). The results of TTC staining and MRI indicated that ATRA treatment decreases the brain ischemic area caused by CIR injury. (Figs. 1, 2).

ATRA Reduces BBB Permeability and Brain Edema Induced by CIR Injury

The effects of ATRA treatment on CIR induced BBB disruption were investigated. The brain water content in the CIR group was significantly higher than in the sham group, whereas the brain water content in the ATRA treatment (10 and 30 mg/kg) was reduced toward baseline (Fig. 3c,

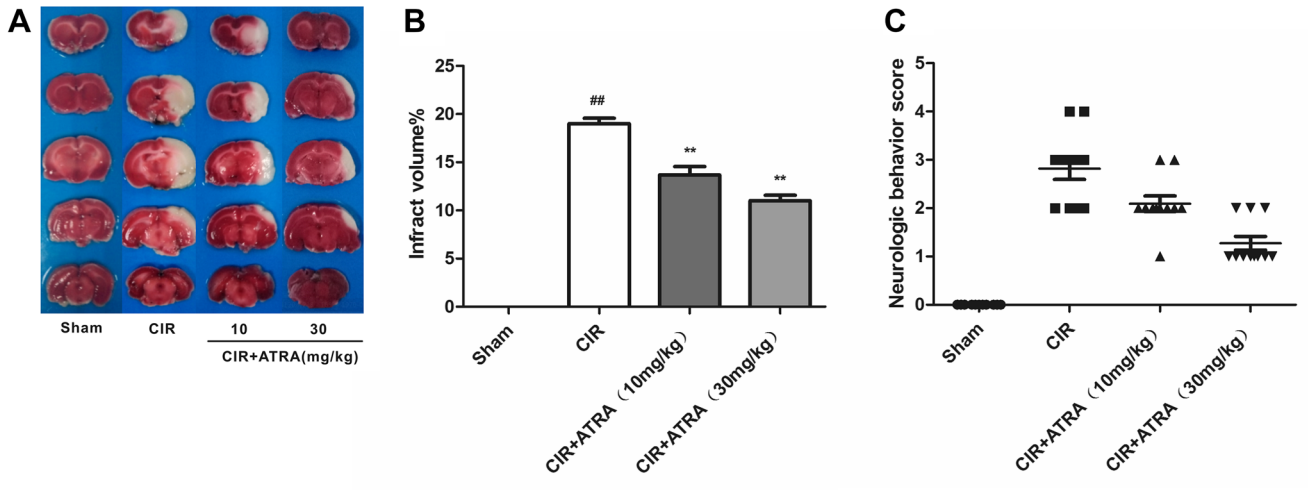

Fig. 1 The cerebral infarct volume and neurological function in different groups. **a** TTC-staining of brain slices (n = 11 in each group, 2 mm for each scale). **b** Quantitative analysis of cerebral infarct volume; **c** quantitative analysis of neurological function (n = 11 in each group). *Sham* sham-operated group, *CIR* cerebral ischemia–reperfusion group. $^{\#\#}p < 0.01$ versus Sham group; **P < 0.01 versus CIR group

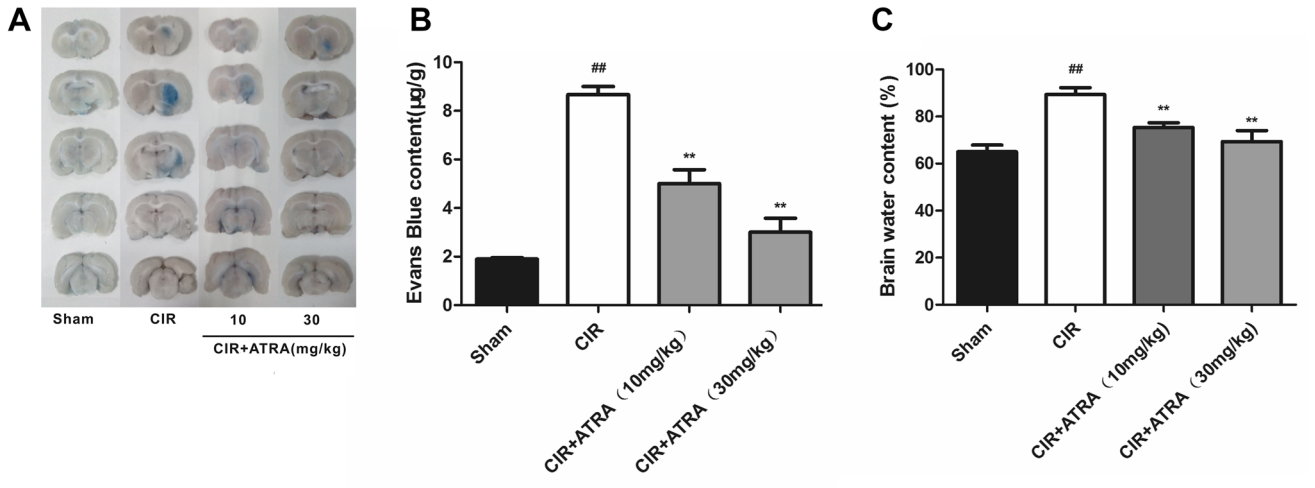

Fig. 2 T1-weighted magnetic resonance imaging (MRI). **a** Representative MRI images from the different groups. The yellow arrows point to the signal intensity-enhanced regions with larger regions and more pronounced signal intensities indicating more serious brain damage. **b** T1 signal intensity enhancement in different groups (n = 5 in each group). *Sham* sham-operated group, *CIR* cerebral ischemia–reperfusion group. $^{\#\#}p < 0.01$ versus Sham group; **P < 0.01 versus CIR group

**p < 0.01). These data suggest that ATRA treatment (10 and 30 mg/kg) can significantly reduce brain edema after CIR injury.

To further determine whether ATRA can maintain BBB integrity after CIR injury, we measured the BBB permeability with Evans blue staining. We also found that Evans blue intensity was significantly increased 24 h after CIR (Fig. 3a, b, $^{\#\#}P < 0.01$), while ATRA treatment (10 and 30 mg/kg) exhibited a significantly lower brain Evans blue intensity (Fig. 3a, b, **p < 0.01).

ATRA Improves Focal Ischemia-Induced Blood–Brain Barrier Injury

The I/R group resulted significant tight junction protein degradation 24 h afte rCIR. However, compared with the CIR group, ATRA administration dramatically attenuated these BBB structural damages. Western blot analysis showed that ATRA significantly reduced tight junction protein degradation and the expression of AQP-4 protein (Fig. 4, **p < 0.01). Additionally, TEM analysis showed less

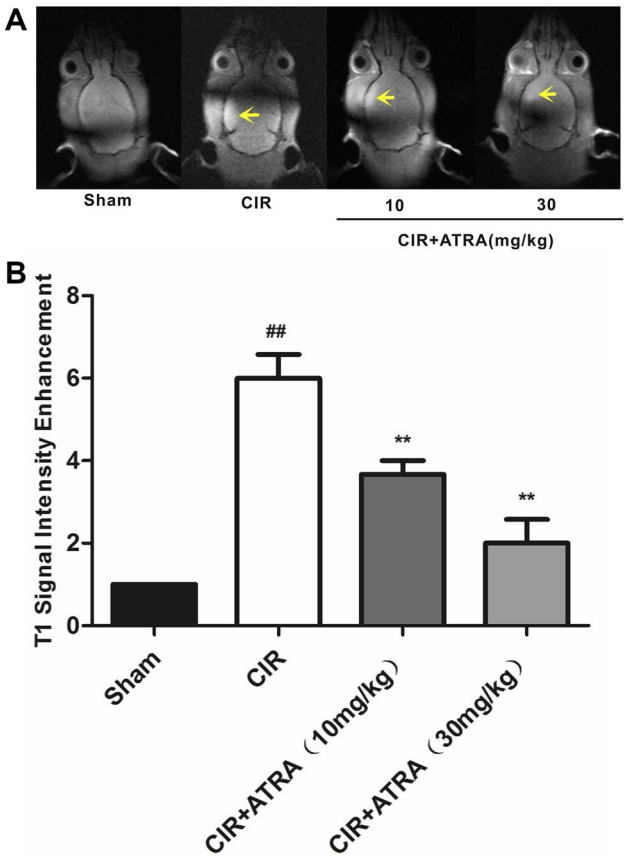

Fig. 3 Determination of blood brain barrier permeability in different groups. **a** Evans blue brain surface photography results (n = 11 in each group, 2 mm for each scale). **b** The content of Evans blue extraction method for quantitative ischemic cerebral hemisphere exudation by formamide (n = 11 in each group). **c** The brain water content of the cerebral hemisphere in the ischemic side was calculated by the wet and dry gravity method in each group (n = 10 in each group). $^{\#\#}p < 0.01$ versus Sham group; $^{**}P < 0.01$ versus CIR group

vacuolations and TJ disruption between endothelial cells in the ATRA treatment (30 mg/kg) group comparison with the CIR group (Fig. 5). The result show that the claudin-5 protein decreased significantly after CIR 24 h, and vascular rupture occurred. However, the ATRA treatment (30 mg/kg) group can significantly reduce the decrease of claudin-5 (Fig. 6). Moreover, the Bax and Cleaved Caspase-3 levels was dramatically decreased by ATRA administration 24 h after CIR (Fig. 7a, b, d, $^{**}p < 0.01$). In contrast to Bax, Bcl-2 levels were significantly increased by ATRA treatment when compared with the I/R group rat (Fig. 7a, c, $^{*}p < 0.05$, $^{**}p < 0.01$). Therefore, we confirmed that ATRA treatment could indeed provide neuroprotective effects by relieving BBB disruption early after CIR.

ATRA Decreases MMP-9 Enzyme Activity and Protein Expression Following CIR Injury

To investigate whether ATRA can exert MMP-9 enzyme activity and protein expression inducd by CIR injury, gelatin zymography assay and western blot pictures were analyed. MMP-9 enzyme activity and protein levels were significantly increased in rats that underwent CIR, ATRA treatment effectively reduced levels of MMP-9 enzyme activity and protein, suggesting that ATRA improves BBB integrity through modulatiing MMP-9 level (Fig. 8, $^{**}p < 0.01$).

ATRA Reduces Phosphorylation of JNK and P38 after CIR Injury

To elucidate the effect of ATRA on MAPK signaling pathway, we assessed phosphorylated JNK (p-JNK) and P38 (p-P38) by western blot. As depicted in Fig. 9, the expression of total JNK and P38 in the brain ischemic area was comparable among different groups. Expression of p-JNK and p-P38 was significantly increased in MCAO rats 24 h after CIR compared with the sham-operated group (Fig. 9a–c, $^{\#\#}p < 0.01$). Administration of ATRA (10 and 30 mg/kg) significantly reduced the expression of p-JNK and p-P38 compared to the MCAO rats 24 h after CIR (Fig. 9a–c, $^{**}p < 0.01$). The results also showed that after CIR by retinoic acid receptor alpha (RARα) content decreased. However, ATRA can reduce the damage of RARα (Fig. 9a, d, $^{**}p < 0.01$).

Effects of Retinoic Acid Alpha Receptor Inhibitors Ro41-5253 and JNK/P38MAPK Signal Pathway Inhibitor SB203580/SP600125 on CIR Injury in Rat

To further investigate the effect of ATRA on brain damage induced by CIR, retinoic acid alpha receptor inhibitors Ro41-5253 and JNK/P38MAPK signal pathway inhibitor SB203580/SP600125 were administrated before CIR. As showed in Fig. 10, compared with CIR + H group, CIR + Ro + H group could reverse the protective effect of ATRA on CIR injury (Fig. 10, $^{\&}p < 0.05$, $^{\&\&}p < 0.01$). While JNK/P38MAPK signal pathway inhibitor SB203580/SP600125 dramatically decreased the neurologic deficit score, brain water content, infarct volume and Evans blue content compared with CIR group (Fig. 10, $^{*}p < 0.05$, $^{**}p < 0.01$), These results indicated that JNK/P38MAPK signal pathway inhibitor can reduce the injury of CIR in rats.

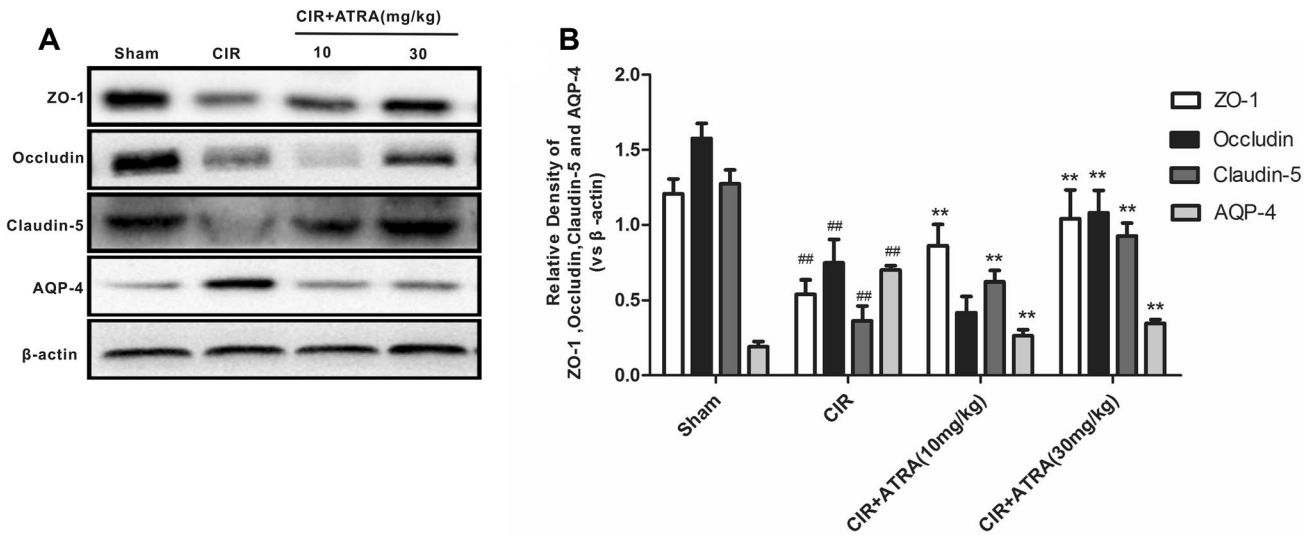

Fig. 4 The expression of tight junction proteins and aquaporin-4 in each group. **a, b** ZO-1, occludin, claudin-5, AQP-4 protein expression levels in the ischemic zone of the rat brain were determined by western blotting and densitometric analysis with β-actin used as an internal control (n = 12 in each group). $^{\#\#}p < 0.01$ versus sham group; $^{**}P < 0.01$ versus CIR group; $^{*}P < 0.05$ versus CIR group

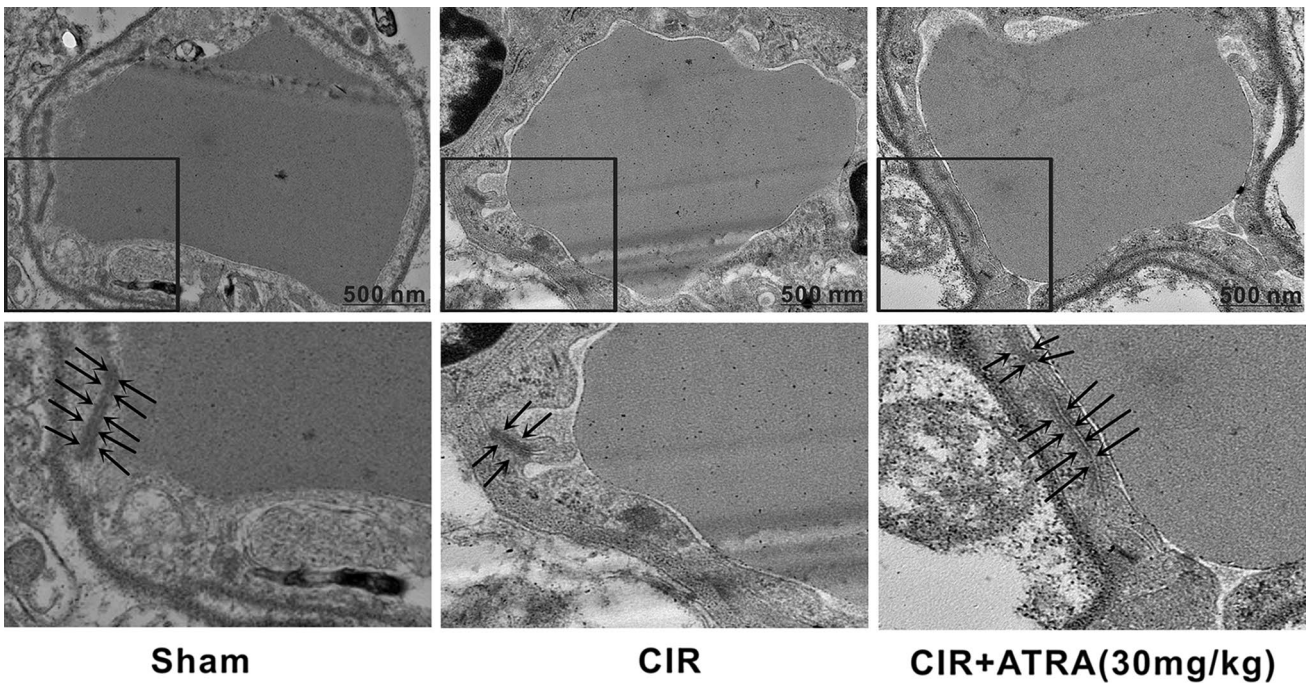

Fig. 5 Morphological observation of tight junction under transmission electron microscopy. Representative transmission electron microscopy images of tight junction structure changes in the ischemia reperfusion zone in the rat brain (n = 5 in each group). Scale bar 500 nm

Discussion

The loss of BBB integrity greatly influences the events after CIR, and this loss is directly related to brain edema and neuro-functional impairment. ATRA, which is an active metabolite of vitamin A, mediates most of the biological functions of vitamin A. Previous studies have found that retinoic acid plays an important role in the formation of blood–brain barrier [22]. In this present study, we demonstrated that ATRA administration significantly reduces neurological score, cerebral infract volume, brain water content and BBB disruption as evidenced by EB staining

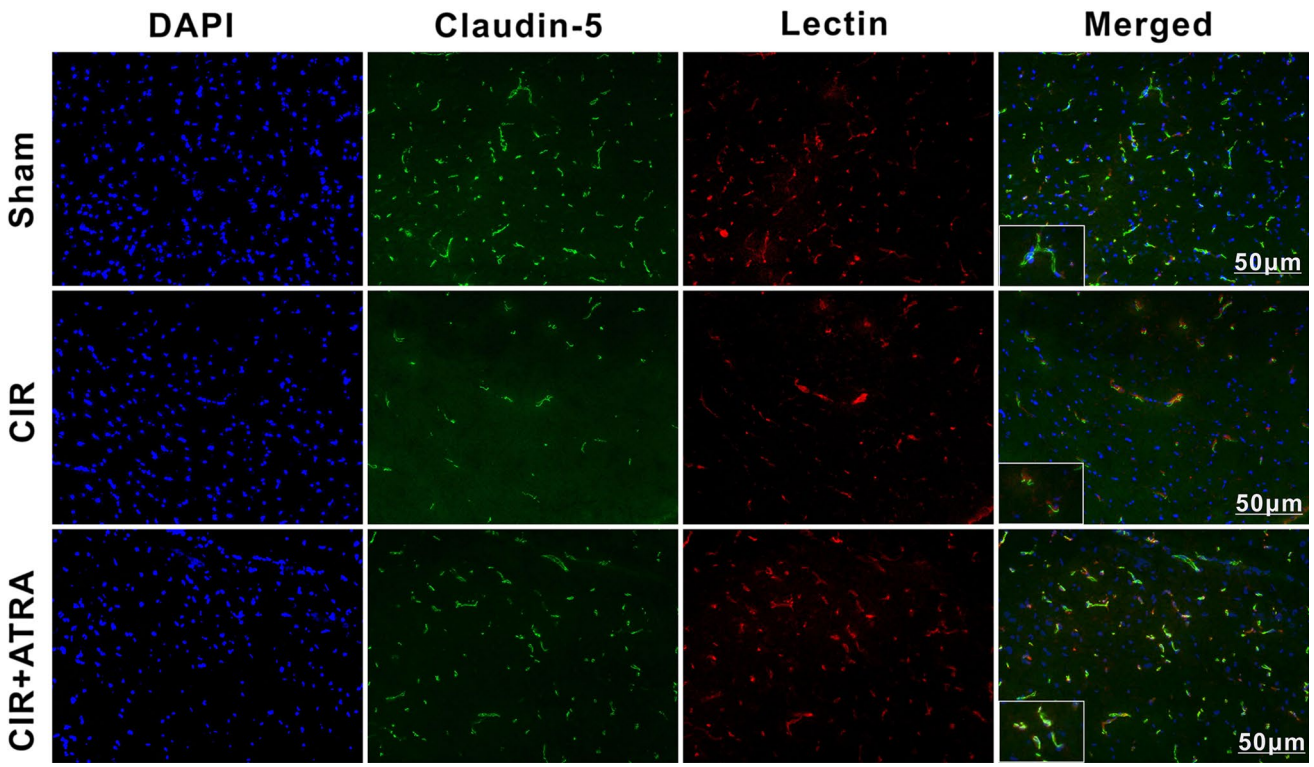

Fig. 6 Changes of tight junction protein claudin-5 expression in brain during middle cerebral artery occlusion in SD rats. Detection of claudin-5 in cerebral ischemia reperfusion area by immunofluorescence assay (n = 5 in each group). Scale bar 50 μm

and Omniscan extravasation after CIR, supporting the neuroprotective properties of this drug. We also found that ATRA treatment reduced the expression and activity of MMP-9,AQP-4 p-JNK and p-P38, increased claudin-5, occludin and ZO-1 expression after CIR. Furthermore, retinoic acid alpha receptor antagonist Ro 41-5253 showed no statistically neuroprotective effect after CIR; however, JNK/P38MAPK signal pathway inhibitor SB203580/SP600125 showed significantly neuroprotective effect after CIR. Compared with the CIR group. ATRA administration significantly reduced the expression of p-JNK and p-P38. These results suggest that the therapeutic effects of ATAR in modulating BBB integrity post-CIR injury may be associated with the dru's effect on JNK/P38 MAPK Pathway. In this study, ATRA (30 mg/kg) can significantly reduced the infarct volume and the evans blue content, indicating that ATRA can reduce the damage of blood brain barrier after CIR.

MMPs involved in the degradation of extracellular matrix and the stability of microenvironment [23]. At present, MMP-9 is most closely related to blood–brain barrier damage after cerebral ischemia [6]. Silencing MMP-9 gene can up regulate the expression of tight junction protein occludin and decrease the permeability of blood–brain barrier [24–26]. In acute cerebral ischemia, the expression of MMP-9 in brain tissue increased significantly, MMP-9 through the close connection between the basement membrane and blood brain barrier degradation of endothelial cells, loss of the blood–brain barrier in the pathological process of cerebral ischemia development [7]. This research showed that the expression and activity of MMP-9 increased after 24 h of CIR injury, the expression of MMP-9 in the ischemic infarct area of ATRA 10 and 30 mg/kg groups was significantly less, suggesting that the protective effect of blood–brain barrier may be related to the decrease of MMP-9 activity. It has been proved that retinoic acid alpha receptor (RARα) are expressed in both smooth muscle cells and endothelial cells of cerebral vascular system. Studies have shown that binding of retinoic acid to RAR and activation of RAR with retinoic acid responsive elements (RARE) located on the promoter can promote the expression of tissue inhibitor of metalloproteinases (TIMPS). Regulating the ratio of MMPs/TIMP and decreasing the expression of MMP-9. ATRA can also promote the expression of nuclear repressor NF kappa B, and the expression of MMP-9 can be inhibited by the combination of NF kappa B and MMP-9 promoter [27–29]. In normal brain tissue, the expression level of MMP-9 is low, when the cell is stimulated, extracellular matrix (ECM) need to reshape the expression of

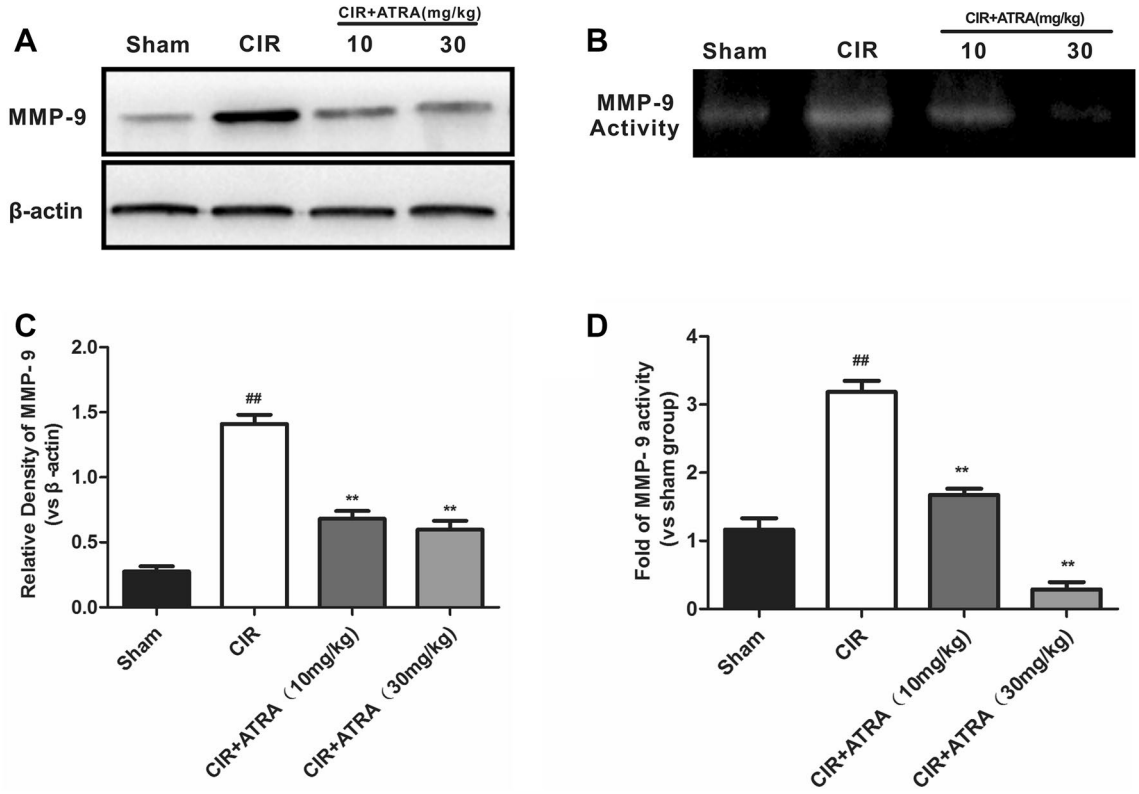

Fig. 7 The expression of apoptosis-related proteins in each group. **a–d** Bax, Bcl-2, cleaved caspase-3 protein expression levels in the ischemic zone of the rat brain were determined by western blotting and densitometric analysis with β-actin used as an internal control (n = 12 in each group). $^{\#\#}p < 0.01$ versus Sham group; $^{**}P < 0.01$ versus CIR group; $^{*}P < 0.05$ versus CIR group

MMP-9 will be increased, the expression regulation by a variety of growth factors and cytokines, and these factors can often play a role through the activation of MAPK signaling pathway in cells [30]. It has also been found that MMP-9 activated by P38 signaling pathway is involved in TNF-alpha induced destruction of corneal endothelial cell barrier function [31].

Our study found that phosphorylation levels of MAPK signaling pathway proteins JNK and P38 were significantly increased after 24 h of CIR. However, the 10 and 30 mg/kg dose of ATRA significantly inhibited the phosphorylation of JNK and P38, the key proteins of MAPK signaling pathway. These results suggest that the protective effect of ATRA on blood–brain barrier may be related to the inhibition of MAPK signaling pathway. In order to understand the blood brain barrier after CIR injury is regulated by retinoic acid alpha receptor and JNK/P38MAPK signaling pathways, we added retinoic acid alpha receptor antagonist Ro 41-5253. JNK signaling pathway inhibitor SP600125, P38 MAPK signaling pathway inhibitor SB203580 treated by Sham group, CIR group, CIR + H (ATRA, 30 mg/kg) group, CIR + Ro + H (ATRA, 30 mg/kg) group, CIR + SP600125 + SB203580 group to explore JNK/P38MAPK signaling pathway in the blood brain barrier after CIR injury. The results showed that compared with CIR group, given before ischemia SP600125 and SB203580 group was significantly reduced the neurological deficits, brain infarction size, cerebral water content and EB content decreased, indicating inhibition of JNK/P38 signaling pathway can reduce CIR injury. In addition, compared with CIR + H (ATRA, 30 mg/kg) group, CIR + Ro + H group had neurological impairment, increased cerebral infarction volume, increased brain water content and EB content. Combined with Fig. 10, experimental results show that ATRA can promote the expression of RARα, suggests that the protective effect of ATRA on CIR may be related to the activation of RARα Therefore, we can conclude that the role of ATRA in reducing blood–brain barrier loss may be related to the activation of the retinoic acid alpha receptor and inhibition of the JNK/P38 MAPK signaling pathway.

It has been proved that activation of JNK pathway is closely related to neuronal apoptosis [32–37]. In CIR injury, there are excessive activation of JNK, increased expression of JNK protein, and activation of JNK pathway leads to neuronal apoptosis [38]. The determination of Bcl-2 cleaved

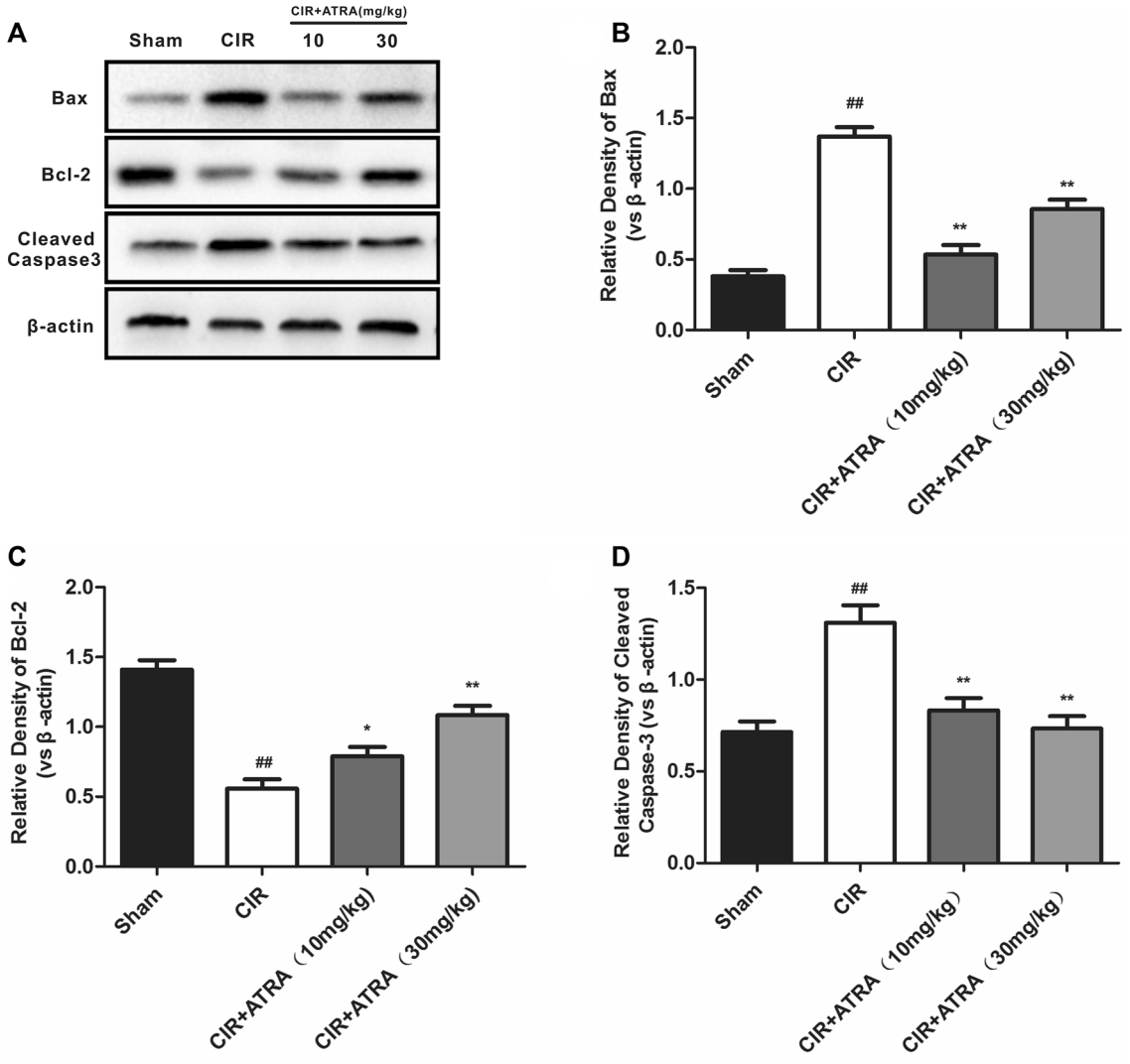

Fig. 8 The protein expression and activity of MMP-9. **a, c** MMP-9 protein expression in the ischemic zone of the rat brain was determined by western blotting (n = 10 in each group). **b, d** MMP-9 activity in the ischemic zone of the rat brain was determined by gelatin zymography (n = 10 in each group). $^{\#\#}p < 0.01$ versus Sham group; $^{**}P < 0.01$ versus CIR group

caspase-3 and Bax in ischemic brain tissue can indirectly reflect the degree of apoptosis in CIR. Our study found that the expression of CIR group Bax and cleaved caspase-3 increased, Bcl-2 expression decreased, showed that after CIR injury, with the activation of the JNK pathway induced apoptosis of neurons. In recent years, other study also confirmed that P38 MAPK pathway involves almost all the physiological function and the process of CIR injury, all signaling link, is involved in the blood–brain barrier injury is one of the most critical path [39]. It is found that P38 MAPK participates in the formation of iNOS under various stimulation conditions [40].The changes and roles of nitric oxide (NO) and nitric oxide synthase (NOS) in cerebral ischemia reperfusion injury have attracted extensive attention. A large amount of NO is produced after cerebral ischemia and reperfusion, in which the regulation of MMP-9 by NO and cGMP is the key [41]. And then promote the development of ischemic brain damage.

Different signaling pathways activate different transcription factors in MAPK, which mediate different biological effects, but there are also extensive cross links among these pathways. Phosphorylation of JNK can promote the formation of its transcription factor c-Jun, and c-Jun can bind to the transcriptional activation protein-1

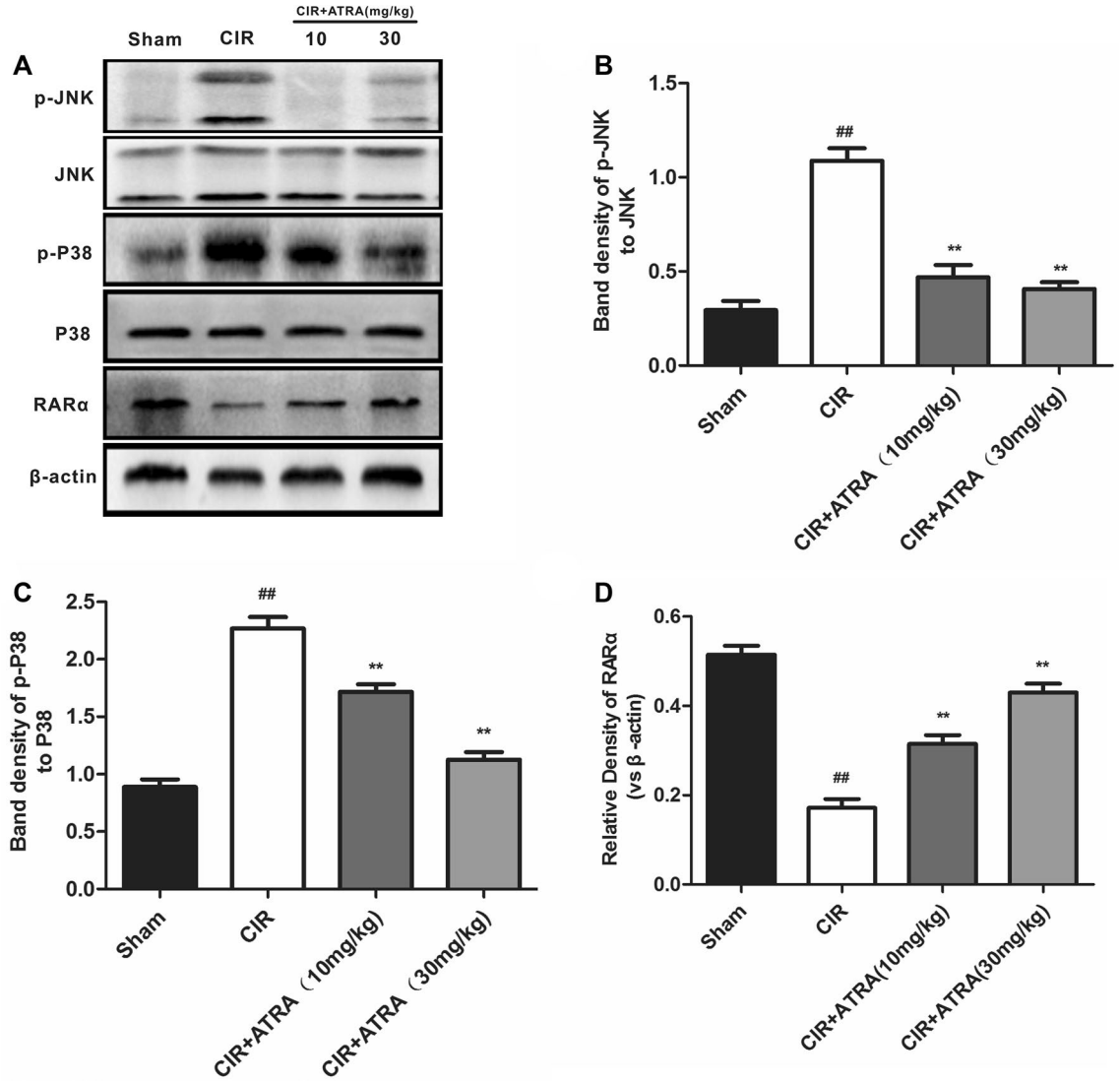

Fig. 9 The expression of JNK/P38 signaling pathway related proteins and RARα in each group. **a** JNK, P38, p-JNK, p-P38 and RARα protein expression levels in the ischemic zone of the rat brain were determined by western blotting (n = 12 in each group). **b–c** Relative bands density of p-JNK to the total-JNK and relative bands density of p-P38 to the total-P38. **d** Relative bands density of RARα to the β-actin. $^{\#\#}p < 0.01$ versus Sham group; $^{**}P < 0.01$ versus CIR group

(AP-1) site of many genes in the posterior region, and phosphorylation of P38MAPK also activates transcription factor AP-1. The MMP-9 promoter contains AP-1 sites, and studies have shown that reducing AP-1 can significantly inhibit the expression of MMP-9 [42, 43]. Therefore, we speculate that the loss of the blood–brain barrier after cerebral ischemia reperfusion, probably through activation of JNK/P38MAPK signaling pathway to the phosphorylation and activation of JNK and P38MAPK to activate downstream MMP-9 promoter AP-1 sites, promote the replication and transcription of MMP-9 resulted in the overexpression and degradation of tight junction proteins and extracellular matrix leading to blood brain barrier damage.

In summary, our results showed that after CIR injury of blood brain barrier in the presence of increased JNK and P38 phosphorylation, MMP-9 content increased. The inhibition of JNK and P38 phosphorylation, can reduce the damage of blood–brain barrier after CIR. In addition, the ATRA administration (30 mg/kg) can reduce CIR injury, the possible mechanism is ATRA by activating retinoic acid alpha receptor, downregulation phosphorylation of JNK, phosphorylation of P38, decrease the content of MMP-9 to produce protective effect. Due to the limitation of experiment time and expense, this experiment only refers to the previous literature research, and does not set a number of time points to observe the changes of each experimental index, which will be further

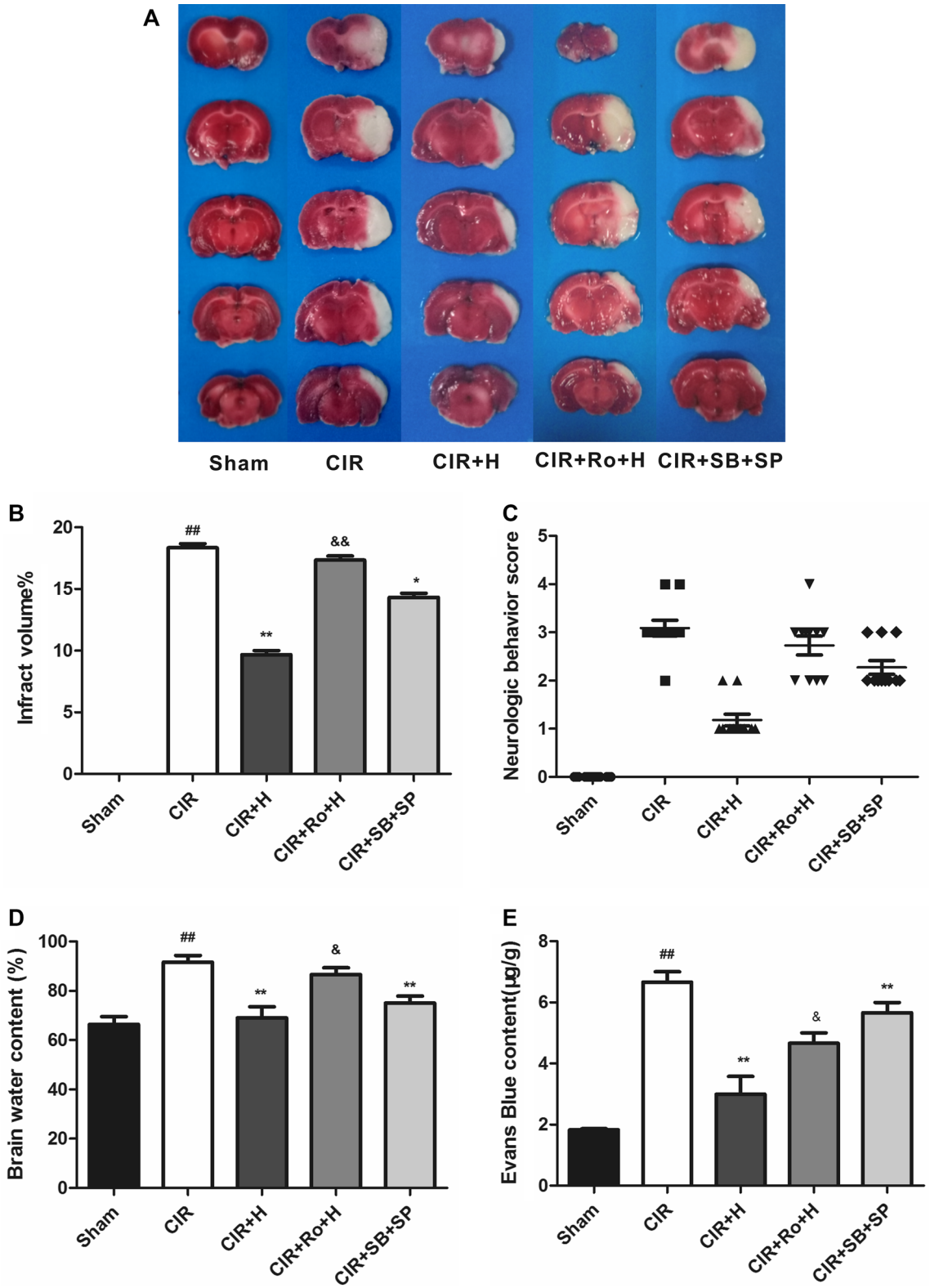

improved in the experiment. In addition, the mechanism by which ATRA inhibits the phosphorylation of JNK and P38, and the resolution of these problems will further elucidate the mechanism of ATRA's protective effect on the blood–brain barrier and provide important research foundations.

◂**Fig. 10** Effects of retinoic acid alpha receptor inhibitors Ro41-5253 and JNK/P38MAPK signal pathway inhibitor SB203580/SP600125 in different groups. **a** TTC-staining of brain slices (n = 11 in each group, 2 mm for each scale). **b** Quantitative analysis of cerebral infarct volume. **c** Quantitative analysis of neurological function (n = 11 in each group). **d** The brain water content of the cerebral hemisphere in the ischemic side was calculated by the wet and dry gravity method in each group (n = 11 in each group). **e** The Evans blue content of the cerebral hemisphere in the ischemic side in each group (n = 11 in each group). *Sham* sham-operated group; *CIR* cerebral ischemia–reperfusion group; CIR + H = 30 mg/kg ATRA-pretreated CIR group; CIR + Ro + H = Ro41-5253 + 30 mg/kg ATRA-pretreated CIR group; CIR + SB + SP = SB203580 + SP600125-treated CIR group. $^{\#\#}p < 0.01$ versus Sham group; $^{**}P < 0.01$ versus CIR group; $^{*}P < 0.05$ versus CIR group; $^{\&\&}P < 0.01$ versus CIR + H group; $^{\&}P < 0.05$ versus CIR + H group

Acknowledgements This study was supported financially by the China and Chongqing Science and Technology Commission (KJ1600235) and Chongqing Science and Technology Commission (CSTC2016jcyj A0268). The funders had no role in the study design, data collection and analysis, decision to publish or preparation of the manuscript.

Compliance with Ethical Standards

Conflict of interest The authors declare that no competing interests exist.

References

1. Kaisar MA, Sajja RK, Prasad S (2017) New experimental models of the blood brain barrier for CNS drug discovery. Expert Opin Drug Discov 12:89
2. Aranda JM, Befeler B, Castellanos (1976) A.BBB and H-V prolongation. Circulation 54:846–847
3. Luissint AC (2012) Tight junctions at the blood brain barrier: physiological architecture and disease associated dysregulation. Fluids Barriers CNS 9:23
4. Liang K, Yue W, Xiao Jing W (2015) Retinoic acid ameliorates blood brain barrier disruption following ischemic stroke in rats. Pharmacol Res 99:125–136
5. Laskowitz DT, Kasner SE, Saver J (2009) Clinical usefulness of a biomarker-based diagnostic test for acute stroke: the biomarker rapid assessment in Ischemic Injury (BRAIN) study. Stroke 40:77
6. Rosenberg GA, Estrada EY, Dencoff JE (1998) Matrix metalloproteinases and TIMPs are associated with blood-brain barrier opening after reperfusion in rat brain. Stroke 29(10):2189–2195
7. Fujimura M, Gasche Y, Morita Fujimura Y (1999) Early appearance of activated matrix metalloproteinase-9 and blood-brain barrier disruption in mice after focal cerebral ischemia and reperfusion.Brain Res 842:92–100
8. Turner RJ, Sharp FR (2016) Implications of MMP9 for blood brain barrier disruption and hemorrhagic transformation following ischemic stroke. Front Cell Neurosci 10:56
9. Asthagiri AR, Lauffenburger DA (2010) A computational study of feedback effects on signal dynamics in a mitogen activated protein kinase. Biotechnol Prog 17:227–239
10. Lourenoco SV, Lima DM (2007) Pleomorphic adenoma and adenoid cystic carcinoma: in vitro study of the impact of TGFbeta1 on the expression of integrins and cytoskeleton markers of cell differentiation. Int J Exp Pathol 88:191–198
11. Baker JE (2004) Oxidative stress and adaptation of the infant heart to hypoxia and ischemia. Antioxid Redox Signal 6:423–429
12. Meestersmoor MA, Janssen MJFW, Haar WMT (2011) The ETS Family member TEL binds to nuclear receptors RAR and RXR and represses gene activation. PLoS ONE 6:e23620
13. Zhou TB, Qin YH (2012) The potential mechanism for the different expressions of gelatinases induced by all trans retinoic acid in different cells. J Recept Signal Transduct Res 32:129–133
14. Liu PT, Krutzik SR, Kim J (2005) All-trans retinoic acid down-regulates TLR2 expression and function. J Immunol 174:2467
15. Rao J, Zhang C, Wang P (2010) All trans retinoic acid alleviates hepatic ischemia/reperfusion injury by enhancing manganese superoxide dismutase in rats. Biol Pharm Bull 33:869
16. Rao J, Qian X, Wang P (2013) All-trans retinoic acid preconditioning protects against liver ischemia/reperfusion injury by inhibiting the nuclear factor kappa B signaling pathway. J Surg Res 180(2):e99
17. Zea Longa Z, Weinsten PR, Carlson S (1989) Reversible middle cere bral artery occlusion without craniectomy in rats. Stroke 20:84–91
18. Kim JH, Yu KS, Jeong JH (2013) All trans retinoic acid rescues neurons after global ischemia by attenuating neuroinflammatory reactions. Neurochem Res 38:2604–2615
19. Wang Z, Kou D, Li Z (2014) Effects of propofol dexmedetomidine combination on ischemia reperfusion induced cerebral injury. Neurorehabilitation 35:825–834
20. Lu XY, Wang HD, Xu JG (2015) Deletion of Nrf2 exacerbates oxidative stress after traumatic brain injury in mice. Cell Mol Neurobiol 35:1–9
21. Xu L, Cao F, Xu F (2015) Bexarotene reduces blood-brain barrier permeability in cerebral ischemia-reperfusion injured rats. PLoS ONE 10:e0122744
22. Mizee MR, Wooldrik D, Lakeman KA (2013) Retinoic acid induces blood brain barrier development. J Neurosci 33:1660–1671
23. Romanic AM, White RF, Arleth AJ (1998) Matrix metalloproteinase expression increase after cerebral focal ischemia: inhibition of matrix metalloproteinase-9 reduces infarct size. Stroke 29:1020–1030
24. Huang W, Chen L, Zhang B (2014) PPAR agonist-mediated protection against HIV Tat-induced cerebrovascular toxicity is enhanced in MMP-9-deficient mice.J Cereb. Blood Flow Metab 34:646–653
25. Bonoiu A, Mahajan SD, Ye L (2009) MMP-9 gene silencing by a quantum dot-siRNA nanopiex delivery to maintain the integrity of the blood brain barrier. Brain Res 1282:142–155
26. Xu R, Feng X, Xie X (2012) HIV-1 Tat protein increases the permeability of brain endothelial cells by both inhibiting occluding expression and cleaving occluding via MMP-9. Brain Res 1436:13–19
27. Lackey DE, Hoag KA (2010) Vitamin A upregulates matrix metalloproteinase-9 activity by murine myeloid dendritic cells through a nonclassical transcriptional mechanism. J Nutr 140:1502–1508
28. Dutta A, Sen T, Chatterjee A (2010) All-trans retinoic acid (ATRA) downregulates MMP-9 by modulating its regulatory molecules. Cell Adhes Migr 4:409–418
29. Dutta A, Sen T, Banerji A (2009) Studies on multifunctional effect of all-trans retinoic acid (ATRA) on matrix metalloproteinase-2 (MMP-2) and its regulatory molecules in human breast cancer cells (MCF-7). J Oncol 09:627840
30. Hong S, Park KK, Magae J (2005) Ascochlorin inhibit matrix metalloprotrinase-9 expression by suppressing activator protein-1-mediated gene expression through the ERK 1/2 signaling

pathway: inhibitory effects of ascochlorin on the invasion of renal carcinoma cells. J Biol Chem 05:25202–25209
31. Xu L, Wang T, Meng WY (2015) Salinomycin inhibits hepatocellular carcinoma cell in vasion and migration through JNK/JunD pathway mediated MMP-9 expression. Oncol Rep 33:1057–1063
32. Li K, Cao RJ, Zhu XJ (2015) Erythropoietin attenuates the apoptosis of adult neurons after brachial plexus root avulsion by down-regulating JNK phosphorylation and c Jun expression and inhibiting c PARP cleavage. J Mol Neurosci 56:917–925
33. Jan CR, Su JA, Teng CC (2013) Mechanism of maprotiline-induced apoptosis: role of [Ca^{2+}] (i), ERK, JNK and caspase-3 signaling pathways. Toxicology 304:1–12
34. Anand SS, Babu PP (2011) c-Jun N terminal kinases (JNK) are activated in the brain during the pathology of experimental cerebral malaria. Neurosci Lett 488:118–122
35. Lu TH, Tseng TJ, Su CC (2014) Arsenic induces reactive oxygen species caused neuronal cell apoptosis through JNK/ERK mediated mitochondria dependent and GRP78/CHOP regulated pathways. Toxicol Lett 224:130–140
36. Lai B, Pu H, Cao Q (2011) Activation of caspase-3 and c-Jun NH_2-terminal kinase signaling pathways involving heroin-induced neuronal apoptosis. Neurosci Lett 502:209–213
37. Li Y, Wang F, Liu C (2013) JNK pathway may be involved in isoflurane induced apoptosis in the hippocampi of neonatal rats. Neurosci Lett 545:17–22
38. Zhu H, Zhu H, Xiao S (2012) Activation and crosstalk between the endoplasmic reticulum road and JNK pathway in ischemia reperfusion brain injury. Acta Neurochir 154:1197–1203
39. Kovalska M, Kovalska L, Pavlikova M (2012) Intracellular signaling MAPK pathway after cerebral ischemia-reperfusion injury. Neurochem Res 37:1568–1577
40. Kang J, Zhang Y, Cao X, Fan J (2012) Lycorine inhibits lipopolysaccharide-induced iNOS and COX-2 up-regulation in RAW264.7 cells through suppressing P38 and STATs activation and increases the survival rate of mice after LPS challenge. Int Immunopharmacol 12:249–256
41. Ridnour LA, Windhausen AN, Isenberg JS (2007) Nitric oxide regulates matrix metalloproteinase-9 activity by guanylylcyclase-dependent and independent pathways. Proc Natl Acad Sci USA 104:16898–16903
42. Chien ST, Shi MD, Lee YC, Te CC, Shih YW (2015) Galangin a novel dietary flavonoid, attenuates metastatic feature via PKC / ERK singaling pathway in TPA-treated liver cancer HepG2 cells. Cancer Cell Int 15:15
43. Ma X, Liu Y, Wang Q, Chen Y (2015) Tamoxifen induces the development of hernia in mice by activating MMP-2 and MMP-13 expression. Biochim Biophys Acta 1852:1038–1048